

# Dynamical correction to linear Kohn-Sham conductances from static density functional theory

S. Kurth<sup>1,2,3</sup> and G. Stefanucci<sup>4,5,3</sup>

<sup>1</sup>*Nano-Bio Spectroscopy Group, Departamento de Física de Materiales, Universidad del País Vasco UPV/EHU, Centro Física de Materiales CSIC-UPV/EHU, Avenida Tolosa 72, E-20018 San Sebastián, Spain*

<sup>2</sup>*IKERBASQUE, Basque Foundation for Science, E-48011 Bilbao, Spain*

<sup>3</sup>*European Theoretical Spectroscopy Facility (ETSF)*

<sup>4</sup>*Dipartimento di Fisica, Università di Roma Tor Vergata, Via della Ricerca Scientifica 1, 00133 Rome, Italy*

<sup>5</sup>*INFN, Laboratori Nazionali di Frascati, Via E. Fermi 40, 00044 Frascati, Italy*

For molecules weakly coupled to leads the *exact* linear Kohn-Sham (KS) conductance can be orders of magnitude larger than the true linear conductance due to the lack of *dynamical* exchange-correlation (xc) corrections. In this work we show how to incorporate dynamical effects in KS transport calculations. The only quantity needed is the *static* xc potential in the molecular junction. Our scheme provides a comprehensive description of Coulomb blockade without breaking the spin symmetry. This is explicitly demonstrated in single-wall nanotubes where the corrected conductance is in good agreement with experimental data whereas the KS conductance fails dramatically.

PACS numbers: 05.60.Gg, 31.15.ee, 71.15.Mb, 73.63.-b

The active field of molecular electronics [1] remains a challenge for *ab initio* methods. Density Functional Theory (DFT) is at present the only viable route for an atomistic description of complex molecular junctions. Nevertheless, DFT transport calculations still suffer from some practical difficulties. The fundamental sources of error in the linear conductance are the DFT exchange-correlation (xc) potential used to determine the Kohn-Sham (KS) conductance  $G_s$  and the dynamical xc correction [2–5] predicted by time-dependent (TD) DFT [6] (see Eq. (9) below). Assessing their importance and mutual interplay is especially thorny in weakly coupled molecules where level alignment and charging effects play a prominent role. Toher et al. [7] and Koentopp et al. [4] showed that  $G_s$  evaluated with an accurate, and hence discontinuous [8], xc potential is suppressed, thus capturing the Coulomb blockade (CB) effect at even electron numbers  $N$  (closed shell). This may suggest the dynamical xc correction to be small. However, at odd  $N$  (open shell)  $G_s$  can be orders of magnitude larger than the true conductance  $G$ , even when the *exact* xc potential is employed [10]. A satisfactory “DFT explanation” of CB is, therefore, currently missing. In this Letter we provide a comprehensive picture of CB, valid for all  $N$  without breaking the spin symmetry. The key ingredient is the dynamical xc correction which, remarkably, can be expressed exclusively in terms of *static* DFT quantities. We propose a practical scheme to calculate  $G$  and demonstrate its validity by comparison with recent experiments on single-wall nanotubes.

At zero temperature and when transport is dominated by a single resonance (open shell)  $G_s = G$  due to the Friedel sum rule [9]. In this regime  $G$  exhibits a Kondo plateau (no CB peaks) and the discontinuity is essential

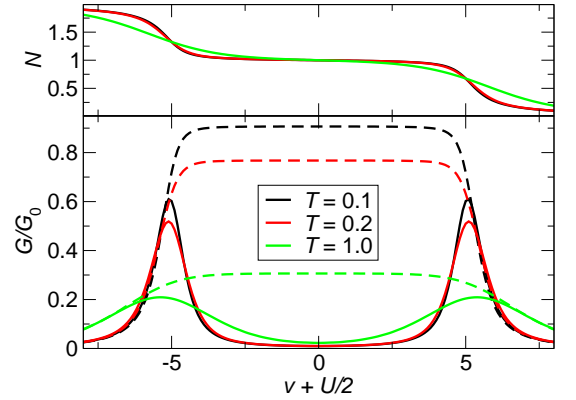


FIG. 1. Top: Electron number  $N$  versus gate in MB and DFT (indistinguishable) for a single level coupled to featureless leads with  $U = 10$ ,  $\mu = 0$  at various temperatures  $T$  (all energies in units of  $\gamma$ ). For these parameters  $T_K = \sqrt{U\gamma} \exp(-\frac{\pi U}{8\gamma}) \simeq 0.06$ . Bottom:  $G$  from Eq. (2) (solid) and  $G_s$  from Eq. (4) (dashed) in units of  $G_0 = 2e^2/h$ .

for  $G_s$  to reproduce the plateau [10–12]. At temperatures higher than the Kondo temperature  $T_K$ , the exact discontinuous xc potential gives instead a  $G_s \gg G$  [10]. To understand this discrepancy we model the resonance with a single level (HOMO or LUMO) of energy  $v$  and Coulomb repulsion  $U$  coupled to left ( $L$ ) and right ( $R$ ) featureless leads contributing  $\gamma = \gamma_L + \gamma_R$  to the broadening of the spectral peaks. Given the Many-Body (MB) spectral function  $A(\omega)$  the number of electrons is

$$N = 2 \int f(\omega) A(\omega), \quad \int \equiv \int \frac{d\omega}{2\pi} \quad (1)$$

whereas the linear (zero-bias) conductance reads

$$G = -2 \frac{\gamma_L \gamma_R}{\gamma} \int f'(\omega) A(\omega) \quad (2)$$

with the Fermi function  $f(\omega) = 1/(e^{\beta(\omega-\mu)} + 1)$  at inverse temperature  $\beta = 1/T$  and chemical potential  $\mu$ . At  $T \gg T_K$  the Abrikosov-Suhl (AS) resonance is suppressed and the spectral function is well represented by [13]

$$A(\omega) = n L_\gamma(\omega - v - U) + (1 - n) L_\gamma(\omega - v) \quad (3)$$

where  $n = N/2$  and  $L_\gamma(\omega) = \gamma/(\omega^2 + \gamma^2/4)$ . For the KS system the spectral function is  $A_s(\omega) = L_\gamma(\omega - v - v_{\text{Hxc}}[N])$ . The Hartree-xc (Hxc) potential  $v_{\text{Hxc}}$  is such that the number of electrons  $N$  which solves  $N = 2 \int f(\omega) A_s(\omega)$  is the same as in Eq. (1). We obtain  $v_{\text{Hxc}}$  by reverse engineering and find that, as function of  $N$ , it has the shape of a smeared step function (not shown). The smearing is due to the level broadening  $\gamma$  induced by contacting the level to the leads and develops into a true discontinuity (at  $N = 1$ ) only in the limit  $\gamma \rightarrow 0$ , as it should [11, 12]. This  $v_{\text{Hxc}}$  is then used to calculate the KS conductance from

$$G_s = -2 \frac{\gamma_L \gamma_R}{\gamma} \int f'(\omega) A_s(\omega). \quad (4)$$

Despite the fact that the MB and DFT  $N$ - $v$  curves are *identical*, see Fig. 1 top, the CB peaks present in  $G$  are completely absent in  $G_s$ , see Fig. 1 bottom. The physical situation discussed here is distinct from that of Ref. 7 where the discontinuity keeps the HOMO doubly occupied and the LUMO empty when gating the molecule (closed shell). The discontinuity correctly suppresses  $G_s$  at even  $N$  but has the opposite effect at odd  $N$ .

*Dynamical xc effects:* Open-shell molecules in the CB regime are probably the most striking example of the inadequacy of standard DFT transport calculations. Below we derive an exact formula for  $G$  in terms of TDDFT quantities. We take the leads as two jellia (the argument can be generalized to more realistic leads) and choose  $z$  as the longitudinal coordinate so that  $z \rightarrow -\infty$  is in the left lead,  $\alpha = L$ , whereas  $z \rightarrow \infty$  is in the right lead,  $\alpha = R$ . Let  $\delta V^\alpha$  be the variation in the classical potential (external plus Hartree) of lead  $\alpha$ . This perturbation generates a current [2, 4]

$$\delta I = (\delta V^R - \delta V^L + \delta V_{\text{xc}}^R - \delta V_{\text{xc}}^L) G_s \quad (5)$$

where  $\delta V_{\text{xc}}^\alpha = \lim_{t \rightarrow \infty} \lim_{z \rightarrow s_\alpha \infty} \delta v_{\text{xc}}(\mathbf{r}, t)$ ,  $s_{R/L} = \pm$ , is the asymptotic value of the variation of the xc potential  $\delta v_{\text{xc}}$ . From linear-response TDDFT

$$\delta V_{\text{xc}}^\alpha = \int dt' d\mathbf{r}' \lim_{t \rightarrow \infty} \lim_{z \rightarrow s_\alpha \infty} f_{\text{xc}}(\mathbf{r}, \mathbf{r}'; t - t') \delta n(\mathbf{r}', t') \quad (6)$$

where  $f_{\text{xc}}$  is the TDDFT kernel and  $\delta n(\mathbf{r}, t)$  is the density variation. The assumption of a steady state implies that

$f_{\text{xc}} \rightarrow 0$  for  $|t - t'| \rightarrow \infty$  and  $\delta n(\mathbf{r}, t \rightarrow \infty) = s_\alpha \delta n$  for  $\mathbf{r}$  in lead  $\alpha$ . In Eq. (6) the contribution of the molecular region to the spatial integral is negligible in the thermodynamic limit. If we define

$$f_{\text{xc}}^{\alpha\beta} = \int dt' \int_{\text{lead } \beta} d\mathbf{r}' \lim_{z \rightarrow s_\alpha \infty} f_{\text{xc}}(\mathbf{r}, \mathbf{r}'; t') \quad (7)$$

then  $\delta V_{\text{xc}}^\alpha = \sum_{\beta=L,R} f_{\text{xc}}^{\alpha\beta} s_\beta \delta n$ . We emphasize that  $f_{\text{xc}}^{\alpha\beta}$  is not the static DFT kernel since the limit  $t \rightarrow \infty$  is taken *after* the limit  $|z| \rightarrow \infty$  and these two limits, in general, do not commute [14]. This implies that we cannot model  $f_{\text{xc}}^{\alpha\beta}$  by performing DFT calculations on leads of finite length. Inserting the expression for  $\delta V_{\text{xc}}^\alpha$  into Eq. (5) we find  $\delta I = (\delta V^L - \delta V^R) G_s - \Phi G_s \delta n$  where

$$\Phi \equiv f_{\text{xc}}^{RL} + f_{\text{xc}}^{LR} - f_{\text{xc}}^{RR} - f_{\text{xc}}^{LL}. \quad (8)$$

The expression for  $\delta I$  is correctly gauge invariant. The kernel  $f_{\text{xc}}$  is defined up to the addition of an arbitrary function  $q(\mathbf{r}) + q(\mathbf{r}')$  [15] and  $\Phi$  is invariant under this transformation. In conclusion

$$G \equiv \frac{\delta I}{(\delta V^R - \delta V^L)} = \frac{G_s}{1 + \chi \Phi G_s}. \quad (9)$$

The quantity  $\chi \equiv \delta n / \delta I \simeq 1/(v_F \sigma)$  with  $v_F$  the Fermi velocity and  $\sigma$  the cross section of the leads [16]. In the following we define  $\chi \Phi G_s$  as the *dynamical* xc correction since  $\Phi$  is expressed in terms of the TDDFT kernel.

*Approximations to  $\Phi$ :* To gain some insight into the density dependence of  $\chi \Phi$  we consider again the single level model. For  $N \neq 1$  and  $T < \gamma$  the real and KS systems respond similarly and consequently  $G \simeq G_s$ . On the other hand for  $N = 1$  we have  $G \simeq 0$  whereas  $G_s \simeq G_0 = 2e^2/h$  the quantum of conductance. Therefore  $\chi \Phi$  is small for  $N \neq 1$  and large for  $N = 1$ . Interestingly the quantity  $\partial v_{\text{Hxc}} / \partial N$  behaves similarly. Is there any relation between  $\chi \Phi$  and  $\partial v_{\text{Hxc}} / \partial N$ ? If so this relation would simplify enormously the problem of estimating the dynamical xc correction since  $\partial v_{\text{Hxc}} / \partial N$  can be calculated from static DFT. In the following we show that in the CB regime this relation does actually exist.

Consider the system in equilibrium. Using Eq. (1) the compressibility  $\kappa = \partial N / \partial \mu$  can be written as  $\kappa = \frac{\gamma}{\gamma_L \gamma_R} G + 2 \int f(\omega) \partial A(\omega) / \partial \mu$ , where we identified the conductance  $G$  of Eq. (2). If we define the quantity  $R \equiv -2 \int f(\omega) \partial A(\omega) / \partial N$  then  $\kappa = \frac{\gamma}{\gamma_L \gamma_R} G / (1 + R)$ . As the MB and DFT densities are the same, the MB and DFT compressibilities are the same too. Hence  $\kappa = \frac{\gamma}{\gamma_L \gamma_R} G_s + 2 \int f(\omega) \partial A_s(\omega) / \partial \mu$ , where we identified the KS conductance  $G_s$  of Eq. (4). The KS spectral function depends on  $\mu$  through  $N$ , and the dependence on  $N$  is all contained in  $v_{\text{Hxc}}$ . Since  $\frac{\partial A_s}{\partial v_{\text{Hxc}}} = -\frac{\partial A_s}{\partial \omega}$  (see definition of  $A_s$  below Eq. (3)) we have  $\frac{\partial A_s}{\partial \mu} = -\frac{\partial A_s}{\partial \omega} \frac{\partial v_{\text{Hxc}}}{\partial N} \frac{\partial N}{\partial \mu}$ . Using this result under the integral, solving for  $\kappa$  and

equating the MB and DFT expressions one easily obtains

$$\frac{G}{G_s} = \frac{1+R}{1 + \frac{\gamma}{\gamma_L \gamma_R} G_s \frac{\partial v_{\text{Hxc}}}{\partial N}}. \quad (10)$$

No approximations have been made so far. Let us study the dependence of  $R$  on temperature.

We first consider the low temperature case. For simplicity we take  $\gamma_L = \gamma_R$  and set  $v = -U/2$  at the particle-hole (ph) symmetric point (half-filling). At zero temperature  $G = G_s = G_0$  and hence  $R = R_0 \equiv \frac{4G_0}{\gamma} \frac{\partial v_{\text{Hxc}}}{\partial N}$  [17]. For temperatures  $T > T_K$  the AS resonance broadens and its height decreases as  $h(T/T_K)$  where  $h$  is a universal function which approaches zero at high  $T$  [21]. This means that  $R \simeq h(T/T_K)R_0$  remains large until the AS resonance disappears. No simple relation between  $\Phi$  and  $\partial v_{\text{Hxc}}/\partial N$  exists when Kondo correlations are present.

At temperatures  $T \gg T_K$  thermal fluctuations destroy the Kondo effect and the MB spectral function is well approximated by Eq. (3). Therefore  $R(v) = I(v) - I(v+U)$  where  $I(E) \equiv \int f(\omega) L_\gamma(\omega - E)$ . We can derive a more convenient expression for  $R$  by inserting Eq. (3) into Eq. (1) to find

$$N = \frac{2I(v)}{1 + I(v) - I(v+U)}, \quad (11)$$

and hence  $1+R = 2I(v)/N$ . Unfortunately  $I(v)$  is not an explicit function of  $N$  due to the implicit dependence of  $v = v[N]$ . However, for  $v < \mu$ , or equivalently for  $N < 1$ , we have  $I(v+U) \ll 1$ . Thus for  $N < 1$  we can write  $N \simeq 2I(v)/(1 + I(v))$  from which we infer  $I(v) \simeq N/(2 - N)$ . Using ph symmetry we therefore approximate  $R$  by the explicit function  $1+R = 2/(1 + |\delta N|)$  where  $\delta N = N - 1$ . Inserting this into Eq. (10) we deduce the main result of this Letter

$$\frac{G}{G_s} = \frac{2}{1 + |\delta N|} \frac{1}{1 + \frac{\gamma}{\gamma_L \gamma_R} G_s \frac{\partial v_{\text{Hxc}}}{\partial N}}. \quad (12)$$

Equation (12) provides a simple and implementable formula to correct the KS conductance. In fact, the dynamical xc correction of Eq. (9) is entirely expressed in terms of *static* DFT quantities. Moreover, whereas  $\Phi$  involves the TDDFT kernel with coordinates in the *leads* the correction in Eq. (12) involves only the DFT  $v_{\text{Hxc}}$  in the *molecular junction*. The accuracy of Eq. (12) is examined in Fig. 2, and benchmarked against the MB conductance of Eq. (2). Even though the approximate  $R$  is not on top of the exact one, see inset, the agreement between the two conductances is extremely good. The position, width and height of the peaks as well as the decay for large  $|v|$  are all well reproduced. Most importantly the plateau of  $G_s$ , see Fig. 1, is completely gone.

*Application to physical systems:* In real molecules  $v_{\text{Hxc}}$  is a  $\mathbf{r}$ -dependent functional of the density. We

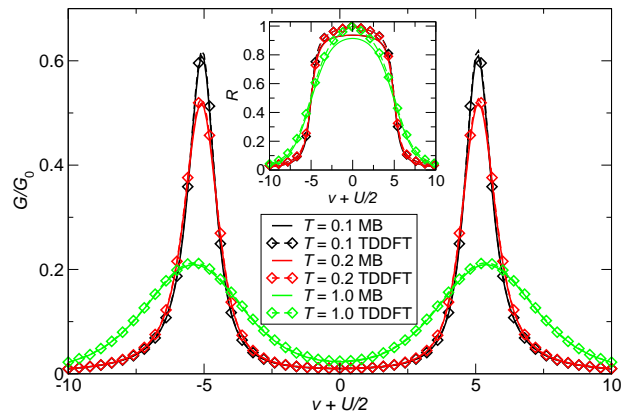


FIG. 2. Linear conductance from Eq. (2) using the spectral function Eq. (3) (MB, solid) and from Eq. (12) (TDDFT, dashed). The inset shows a comparison between the exact and the approximate  $R$ . Same parameters as in Fig. 1.

write  $v_{\text{Hxc}}(\mathbf{r}) = \delta v_{\text{Hxc}}(\mathbf{r}) + \bar{v}_{\text{Hxc}}$  as the sum of a functional  $\delta v_{\text{Hxc}}$  with a weak dependence on  $N = \int_V d\mathbf{r} n(\mathbf{r})$  and a spatially uniform part  $\bar{v}_{\text{Hxc}} = \frac{1}{V} \int_V d\mathbf{r} v_{\text{Hxc}}(\mathbf{r})$ , where the integral is over the volume  $V$  of the molecular junction. For weakly coupled molecules  $\bar{v}_{\text{Hxc}}$  exhibits sharp steps as function of  $N$  when  $N$  crosses an integer. If we are at resonance and spin fluctuations are suppressed (no Kondo effect) then the KS conductance must be corrected according to Eq. (12) in which  $\partial v_{\text{Hxc}}/\partial N \rightarrow \partial \bar{v}_{\text{Hxc}}/\partial N$ . Below we argue that this correction applies out-of-resonance too. Let  $\mu$  be in the HOMO-LUMO gap and consider a two-level system with  $\Gamma_\alpha$  the  $2 \times 2$  broadening matrix. For general  $\Gamma_\alpha$  no simple analytic relation between  $G$  and  $N$  exists. However if  $\Gamma_{\alpha,ml} = (\gamma_\alpha/2)\delta_{ml}$  then  $N = 2 \int f(\omega) \text{Tr}[A(\omega)]$  and  $G = -2 \frac{\gamma_L \gamma_R}{\gamma} \int f'(\omega) \text{Tr}[A(\omega)]$ . Discarding the dependence of  $\delta v_{\text{Hxc}}$  on  $\mu$  (which is weak by definition) we can go through the same steps of the single-level derivation and find again Eq. (12). It is therefore reasonable to expect that the KS conductance should be corrected even out-of-resonance (closed shell) and that this correction should be proportional to  $G_s \partial \bar{v}_{\text{Hxc}}/\partial N$ .

We here propose a practical scheme to calculate  $G$  from DFT. Given the KS Hamiltonian matrix  $h_{\text{KS},ml} = \delta_{ml}\epsilon_l$  and the broadening matrices  $\Gamma_{\alpha,ml}$  we determine the density and  $G_s$  in the usual manner.  $G$  is then obtained from Eq. (12) where  $\delta N$  is the deviation of  $(N - \text{Int}[N])$  from 1 whereas  $\gamma_\alpha = \gamma_\alpha(N) = \Gamma_{\alpha,HH}$  if  $\mu \simeq \epsilon_H$  (resonance, open shell) and  $\gamma_\alpha(N) = \frac{1}{2}(\Gamma_{\alpha,HH} + \Gamma_{\alpha,LL})$  if  $\mu \simeq \frac{1}{2}(\epsilon_L + \epsilon_H)$  is in the HOMO-LUMO gap (out-of-resonance, closed shell). One could improve the approximation to  $\gamma_\alpha$  using different weights, but the qualitative features of the results are independent of these details.

To appreciate the decisive impact of the dynamical xc correction we consider two paradigmatic junctions in which  $\delta v_{\text{Hxc}}$  can be discarded. For  $\bar{v}_{\text{Hxc}}$  we choose a best

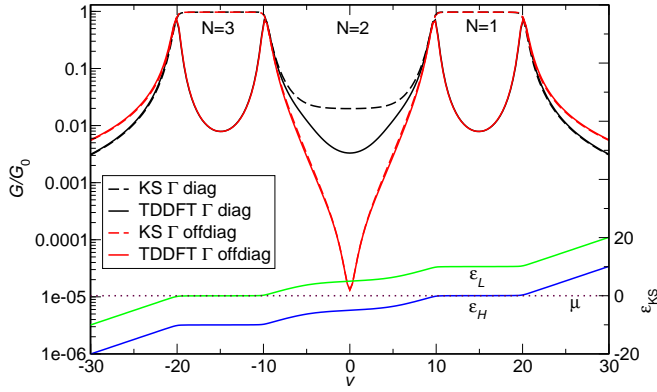


FIG. 3. Linear conductance from Eq. (4) (KS, dashed) and from Eq. (12) (TDDFT, solid) for the HOMO-LUMO model with diagonal and off-diagonal  $\Gamma$ -matrices (left axis) and KS energies  $\epsilon_{H/L} = \epsilon_{0H/L} + \bar{v}_{Hxc}$  (right axis). The electron number  $N$  for different ranges of  $v$  is also indicated.

fit of the zero-temperature limit of the single-level Hxc potential, but now sum over all possible charged states of the molecule [22], i.e.,

$$\bar{v}_{Hxc} = \sum_K \frac{U(K)}{\pi} \arctan\left(\frac{N-K}{W(K)}\right). \quad (13)$$

The charging energies  $U(N)$  are given by the xc part of the derivative discontinuity of the molecule with  $N$  electrons [8]. For the widths we take  $W(N) = 0.16 \gamma(N)/U(N)$  which is consistent with Ref. 19

**HOMO-LUMO model.** We study a two-level system with 2 electrons in the HOMO in the charge neutral state. Let  $\epsilon_{0H} = -\epsilon_{0L} = -\epsilon_0 < 0$  be the noninteracting single-particle energies,

$$\Gamma_L = \Gamma_R = \frac{\gamma}{2} \begin{pmatrix} 1 & 1 \\ 1 & 1 \end{pmatrix}$$

and  $U(N) = U$  independent of  $N$ . We solve the self-consistent equation for the density with  $U = 10$ ,  $\epsilon_0 = 5$ ,  $\mu = 0$  and  $\beta = 10$  (all energies in units of  $\gamma$ ).  $G_s$  and  $G$  from Eq. (12) are shown in Fig. 3 (left axis). As expected the discontinuity of  $v_{Hxc}$  opens a gap in  $G_s$  for even  $N$ , in agreement with the results of Ref. 7. Here the dynamical xc correction only weakly affects  $G_s$  since  $\partial \bar{v}_{Hxc}/\partial N$  is multiplied by  $G_s \ll 1$ . For odd  $N$  the KS conductance exhibits a Kondo plateau due to the pinning of the KS level to  $\mu$ , see right axis. This is the regime previously discussed and no CB is observed. The dynamical xc correction remedies this serious deficiency by correctly suppressing the plateau. The results remain essentially unaltered if the off-diagonal matrix elements of  $\Gamma_\alpha$  are discarded [23].

**SWNT:** Experimental evidence of CB oscillations has recently been reported in metallic single-wall nanotubes

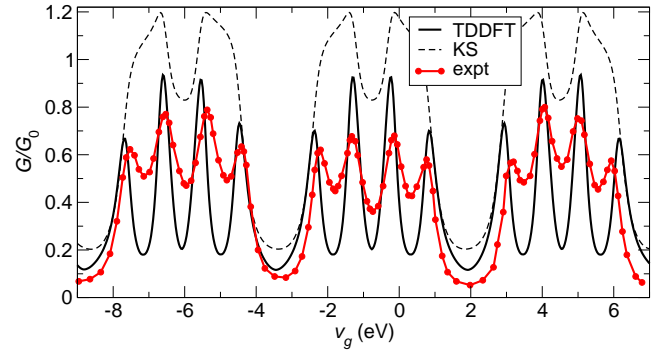


FIG. 4. Linear KS and TDDFT conductance (Eq. (12)) for a SWNT quantum dot in comparison to experimental conductance from Ref. 24, as function of gate voltage  $v_g$ .

(SWNT) quantum dots [24–26]. We now analyze the performance of Eq. (12) in these systems. The finite length of the SWNT causes a level quantization of the twofold degenerate bands. Since the wavevector is a good quantum number our approximation  $\delta v_{Hxc} = 0$  is justified. For a SWNT quantum dot the constant interaction model [27] has been refined by Oreg *et al.* [28] to account for the observed fourfold periodicity in the electron addition energy. We constructed the KS Hamiltonian corresponding to this model and approximated the broadening matrix as  $\Gamma_{\alpha,ml} = (\gamma/2)\delta_{ml}$  [29] (no visible interference [23] from experiment). In Fig. 4 we compare the KS, TDDFT and experimental conductance versus the gate voltage  $v_g$ . We clearly see that the conductance of Eq. (12) correctly exhibits the fourfold periodicity and represents a considerable improvement over  $G_s$  which, instead, shows two deformed Kondo plateaus per period. The qualitative behavior of  $G$  and  $G_s$  does not change by varying the parameters within a reasonable range around the average values reported in Ref. 24.

In conclusion we proposed a practical scheme to correct KS conductances. We highlighted the role of the discontinuity not only for an accurate  $G_s$  but also for an accurate dynamical xc correction to  $G$ . Approaches to generate discontinuous xc potentials are emerging both in the static [30] and dynamical [31] case. Our theory provides a coherent picture of CB within (TD)DFT without breaking the spin symmetry. By application to two different molecular junctions we further showed that the dynamical xc correction always reduces  $G_s$ , thus contributing to close the gap between theoretical predictions and experimental measurements.

S.K. acknowledges funding by the “Grupos Consolidados UPV/EHU del Gobierno Vasco” grant No. IT578-13. G.S. acknowledges funding by MIUR FIRB grant No. RBFR12SW0J. We acknowledge support through travel grants (Psi-K2 4665 and 3962 (G.S.), and Psi-K2 5332 (S.K.)) of the European Science Foundation (ESF).



- 
- [1] G. Cuniberti, G. Fagas and K. Richter, *Introducing Molecular Electronics*, (Springer, Heidelberg, 2005); J.C. Cuevas and E. Scheer, *Molecular Electronics: An Introduction to Theory and Experiment*, (World Scientific, London, 2010).
- [2] G. Stefanucci and C.-O. Almbladh, Phys. Rev. B **69**, 195318 (2004); Europhys. Lett. **67**, 14 (2004).
- [3] N. Sai, M. Zwolak, G. Vignale, and M. Di Ventra, Phys. Rev. Lett. **94**, 186810 (2005).
- [4] M. Koentopp, K. Burke, and F. Evers, Phys. Rev. B **73**, 121403 (2006).
- [5] G. Vignale and M. Di Ventra, Phys. Rev. B **79**, 014201 (2009).
- [6] E. Runge and E. K. U. Gross, Phys. Rev. Lett. **52**, 997 (1984).
- [7] C. Toher *et al.*, Phys. Rev. Lett. **95**, 146402 (2005).
- [8] J. P. Perdew *et al.*, Phys. Rev. Lett. **49**, 1691 (1982).
- [9] H. Mera *et al.*, Phys. Rev. B **81**, 035110 (2010); H. Mera and Y. M. Niquet, Phys. Rev. Lett. **105**, 216408 (2010).
- [10] G. Stefanucci and S. Kurth, Phys. Rev. Lett. **107**, 216401 (2011).
- [11] J. P. Bergfield, *et al.*, Phys. Rev. Lett. **108**, 066801 (2012).
- [12] P. Tröster, P. Schmitteckert and F. Evers, Phys. Rev. B **85**, 115409 (2012).
- [13] See, e.g., H. Haug and A.-P. Jauho, *Quantum Kinetics in Transport and Optics of Semiconductors* (Springer, 2008).
- [14] The static DFT kernel is the response of the *equilibrium*  $v_{xc}$  to a density variation and, deep inside the leads, is determined by the condition of charge neutrality alone.
- [15] This follows from the fact that  $\delta v_{xc}(\mathbf{r}, t \rightarrow \infty)$  is defined up to the addition of an arbitrary constant  $C$ , see also M. Hellgren and E. K. U. Gross, Phys. Rev. A **85**, 022514 (2012).
- [16] A.M. Uimonen *et al.*, Phys. Rev. B **84**, 115103 (2011).
- [17] The compressibility is weakly dependent on temperature up to  $T \simeq \gamma$  [18]. Therefore the  $v_{Hxc}$  obtained by reverse engineering is a good approximation even for  $T = 0$ . At the ph symmetric point ( $N = 1$ ) this approximation gives  $\partial v_{Hxc}/\partial N \sim U^2/\gamma$  [19]. At  $T = 0$  the MB spectral function for  $\omega \simeq \mu$  is dominated by the AS resonance  $A(\omega \simeq \mu) \simeq \frac{4T_K}{\gamma} L_{TK}(\omega - \mu)$  and thus  $\int f(\omega) \frac{\partial A(\omega)}{\partial \mu} \simeq -\frac{2}{\pi\gamma}$ . For the compressibility we have from the Bethe-Ansatz [20]  $\kappa = (8\gamma)/(\pi U^2) [1 + \mathcal{O}(\gamma/U)]$  from which it follows that also  $R$  goes like  $(U/\gamma)^2$ .
- [18] I. Maruyama, N. Shibata and K. N. Ueda, J. Phys. Soc. Jpn **73**, 434 (2004).
- [19] F. Evers and P. Schmitteckert, Phys. Chem. Chem. Phys. **13**, 14417 (2011).
- [20] P. B. Wiegmann and A. M. Tsvelick, J. Phys. C: Solid State Phys. **16**, 2281 (1983).
- [21] T. A. Costi, Phys. Rev. Lett. **85**, 1504 (2000).
- [22] E. Perfetto and G. Stefanucci, Phys Rev B **86**, 081409 (2012).
- [23] This amounts to neglecting interference effects, see G. Stefanucci *et al.*, Phys. Rev. B **79**, 073406 (2009); T. Markussen, R. Stadler and K. S. Thygesen, Nano Lett. **10**, 4260 (2010); J. P. Bergfield *et al.*, Nano Lett. **11**, 2759 (2011).
- [24] W. Liang, M. Bockrath and H. Park, Phys. Rev. Lett. **88**, 126801 (2002).
- [25] M. R. Buitelaar *et al.*, Phys. Rev. Lett. **88**, 156801 (2002).
- [26] S. Sapmaz *et al.*, Phys. Rev. B **71**, 153402 (2005).
- [27] L. P. Kouwenhoven, D. G. Austing, and S. Tarucha, Rep. Prog. Phys. **64**, 701 (2001).
- [28] Y. Oreg, K. Byczuk and B. I. Halperin, Phys. Rev. Lett. **85**, 365 (2000).
- [29] see Supplemental Material for details on the implementation.
- [30] N. A. Lima *et al.*, Europhys. Lett. **60**, 601 (2002); N. A. Lima *et al.*, Phys. Rev. Lett. **90**, 146402 (2003); P. Mori-Sanchez, A. J. Cohen, and W. T. Yang, Phys. Rev. Lett. **102**, 066403 (2009); F. Malet and P. Gori-Giorgi, Phys. Rev. Lett. **109**, 246402 (2012); X. Gao *et al.*, Phys. Rev. B **86**, 235139 (2012); J. Lorenzana, Z.-J. Ying, and V. Brosco, Phys. Rev. B **86**, 075131 (2012); E. Kraisler and L. Kronik, Phys. Rev. Lett. **110**, 126403 (2013).
- [31] C. Verdozzi, Phys. Rev. Lett. **101**, 166401 (2008); S. Kurth *et al.*, Phys. Rev. Lett. **104**, 236801 (2010); D. Hofmann and S. Kümmel, Phys. Rev. B **86**, 201109(R) (2012); P. Elliott *et al.*, Phys. Rev. Lett. **109**, 266404 (2012); S.E.B. Nielsen, M. Ruggenthaler and R. van Leeuwen, EPL **101**, 33001 (2013).

## Supplemental Material

In this Supplemental Material we refer to the paper as I. The many-body Hamiltonian of the SWNT quantum dot was proposed by Oreg et al. (PRL **85**, 365 (2000)) and reads

$$H = \sum_{l\nu\sigma} \epsilon_{0l\nu} n_{l\nu\sigma} + \frac{1}{2} E_C (N - N_0)^2 + \delta U \sum_{l\nu} n_{l\nu\uparrow} n_{l\nu\downarrow} + J N_{\uparrow} N_{\downarrow}. \quad (14)$$

Here  $\sigma$  is the spin index,  $\nu = 0, 1$  is the band index and  $l$  is the integer of the quantized quasi-momentum of the electrons. The Hamiltonian is written in terms of the occupation numbers  $n_{l\nu\sigma}$  since  $N_{\sigma} \equiv \sum_{l\nu} n_{l\nu\sigma}$  (total number of electrons with spin  $\sigma$ ) and  $N = N_{\uparrow} + N_{\downarrow}$  (total number of electrons). The finite length of the SWNT causes a finite subband mismatch  $\delta$  so that the single-particle energies are

$$\epsilon_{0l\nu} = \begin{cases} l\Delta - \delta & \text{for } \nu = 0 \\ l\Delta & \text{for } \nu = 1 \end{cases} \quad (15)$$

with  $\Delta$  the average level spacing. In Eq. (14) the parameter  $E_C$  is the charging energy ( $N_0$  is the number of electrons of the charge neutral SWNT quantum dot),  $\delta U$  is the extra charging energy for two electrons in the same energy level and  $J$  is the exchange energy between electrons of opposite spin. With the parameters of W. Liang et al. (PRL **88**, 126801 (2002)) when an extra electron enters the nanotube it occupies the lowest available single-particle energy level. Thus the *aufbau* is the same as that of the noninteracting Hamiltonian. Accordingly the spin of the ground state is 0, 1/2, 0, 1/2, ... for 0, 1, 2, 3, ... extra electrons. Let  $E(N)$  be the energy of the SWNT with  $N$  extra electrons. Using Eq. (14) it is straightforward to obtain

$$\begin{aligned} E(0) &= 0, \\ E(1) &= \Delta - \delta + \frac{1}{2} E_C, \\ E(2) &= 2\Delta - 2\delta + \frac{1}{2} 4E_C + \delta U + J, \\ E(3) &= 3\Delta - 2\delta + \frac{1}{2} 9E_C + \delta U + 2J, \end{aligned} \quad (16)$$

and so on. The function  $E(N)$  with  $N$  a real continuous variable has a discontinuous derivative at integers  $N$  and the size of this discontinuity is given by  $\Delta(N) = E(N+1) - 2E(N) + E(N-1)$ , see Perdew et al. (PRL **49**, 1691 (1982)). One finds

$$\begin{aligned} \Delta(1) &= E_C + \delta U + J, \\ \Delta(2) &= \delta + E_C - \delta U, \end{aligned} \quad (17)$$

and  $\Delta(N) = \Delta(K)$  if  $N - K = 0 \bmod 2$  with  $K = 1, 2$ . We now turn to the KS system. The KS Hamiltonian of the SWNT has the general form

$$H_{\text{KS}} = \sum_{l\nu\sigma} (\epsilon_{0l\nu} + v_{\text{Hxc}, l\nu}[\{n\}]) n_{l\nu\sigma} \quad (18)$$

The Hxc potential  $v_{\text{Hxc}, l\nu}$  has the property that for a given chemical potential the ground state occupations  $n_{l\nu\sigma}$  of  $H$  and of  $H_{\text{KS}}$  are identical. Since  $H$  is diagonal in the occupation basis and follows the *aufbau* of the noninteracting Hamiltonian, we have that  $v_{\text{Hxc}, l\nu}[\{n\}] = \bar{v}_{\text{Hxc}}[N]$  is uniform and depends only on the total number of particles  $N$ . Thus, for the SWNT the fluctuation  $\delta v_{\text{Hxc}}$  around the average  $\bar{v}_{\text{Hxc}}$  (these quantities have been introduced in ‘‘Application to physical systems’’ of I) is exactly zero. For an isolated SWNT the potential  $\bar{v}_{\text{Hxc}}[N]$  is discontinuous every time  $N$  crosses an integer and the size of the step,  $U$ , is given by the xc part of the discontinuity  $\Delta$ . From Eqs. (17) we find

$$\begin{aligned} U(1) &= E_C + \delta U + J, \\ U(2) &= E_C - \delta U, \end{aligned} \quad (19)$$

and  $U(N) = U(K)$  if  $N - K = 0 \bmod 2$  with  $K = 1, 2$ . The average values of these parameters can be found in W. Liang et al. (PRL **88**, 126801 (2002)). Here we change them slightly to match the peak positions of the SWNT of

length  $\simeq 100$  nm (all energies are in meV):  $\Delta = 9.2$ ,  $\delta = 2.27$ , charging energy  $E_C = 2.485$ , exchange energy  $J = 0.7$ , extra charging energy for doubly occupied levels  $\delta U = 0.37$ . The sharp steps of  $\bar{v}_{\text{Hxc}}$  are smeared when the SWNT is brought in contact with the leads. To find the functional form of  $\bar{v}_{\text{Hxc}}$  we observe that the exact smeared potential which produces the electron number of Fig. 1 of I (single level model) is well approximated by

$$v_{\text{Hxc}}[N] = \frac{U}{2} + \frac{U}{\pi} \arctan\left(\frac{N-1}{W}\right) \quad (20)$$

where  $W \simeq 0.16\gamma/U$ . Therefore a good approximation to the Hxc potential is [cf. with Eq. (13) in I]

$$\bar{v}_{\text{Hxc}}[N] = \sum_K \frac{U(K)}{\pi} \arctan\left(\frac{N-K}{W(K)}\right) \quad (21)$$

where the  $U$ 's are given in Eq. (19). In Eq. (21) we have chosen the smearing parameter  $W(K) = 0.16\gamma(K)/U(K)$  where  $\gamma(K) = \gamma$  is independent of  $K$  since the broadening of the Coulomb blockade peaks observed in W. Liang et al. (PRL **88**, 126801 (2002)) is approximately the same for all peaks (see below). We study the addition and removal of up to 6 electrons from the charge neutral SWNT due to changes of the gate  $v$ . In order to avoid finite-size effects we considered 22 consecutive single-particle levels  $\epsilon_{0l\nu}$ . This ensures that for  $16 \leq N \leq 28$  ( $N_0 = 22$ ) the KS and TDDFT conductances are converged. The broadening of these levels (due to the contacts) is described by the broadening (or hybridization) matrix

$$[\Gamma_\alpha]_{l\nu, l'\nu'} = 2\pi \sum_k T_{k\alpha, l\nu} \delta(\omega - \epsilon_{k\alpha}) T_{k\alpha, l'\nu'} \quad (22)$$

where  $T_{k\alpha, l\nu} = \langle \phi_{k\alpha} | H_{\text{tot}} | \phi_{l\nu} \rangle$  is the matrix element of the lead-SWNT-lead Hamiltonian  $H_{\text{tot}}$  between a bulk eigenstate  $\phi_{k\alpha}$  with energy  $\epsilon_{k\alpha}$  of lead  $\alpha = L, R$  and the eigenstate  $\phi_{l\nu}$  of the SWNT. We discard the off-diagonal matrix elements of the broadening matrix since in the CB regime transport is dominated by a single resonance and interference effects (accounted for by the off-diagonal part of  $\Gamma_\alpha$ ) can be neglected. Furthermore, we take the diagonal matrix elements of  $\Gamma_\alpha$  all the same, which is consistent with the observation below Eq. (21). Thus

$$[\Gamma_\alpha]_{l\nu, l'\nu'} = \delta_{ll'} \delta_{\nu\nu'} \gamma_\alpha \quad (23)$$

with  $\gamma_L = \gamma_R \equiv \gamma/2$ . We solve the self-consistent equation

$$N = 2 \int \frac{d\omega}{2\pi} f(\omega) \text{Tr} [A_s(\omega)] \quad (24)$$

with the KS spectral function

$$[A_s(\omega)]_{l\nu, l'\nu'} = \delta_{ll'} \delta_{\nu\nu'} \frac{\gamma}{(\omega - \epsilon_{0l\nu} - \bar{v}_{\text{Hxc}}[N] - v)^2 + \gamma^2/4} \quad (25)$$

for temperatures  $T < \gamma$ . In Fig. 5 we plot  $\bar{v}_{\text{Hxc}}[N]$  as a function of  $N$  as well as the self-consistent value of  $N$  as a function of  $v_g = v_0 + \alpha v$  for two different values of  $\gamma$ . Here  $v_0$  is chosen in order to have the same reference energy as in W. Liang et al. (PRL **88**, 126801 (2002)) and we estimated the ratio  $\alpha = C/C_g \simeq 250$  between the total capacitance and the gate capacitance from the experimental data. For a given  $v$  we calculate  $A_s$  with  $N = N[v]$  and then the KS conductance from

$$G_s = -\frac{\gamma}{2} \int \frac{d\omega}{2\pi} f'(\omega) \text{Tr} [A_s(\omega)]. \quad (26)$$

Subsequently we calculate  $\partial \bar{v}_{\text{Hxc}} / \partial N$  and correct  $G_s$  according to

$$\frac{G}{G_s} = \frac{2}{1 + |\delta N|} \frac{1}{1 + \frac{\gamma}{\gamma_L \gamma_R} G_s \frac{\partial \bar{v}_{\text{Hxc}}}{\partial N}}, \quad (27)$$

see Eq. (12) of I. In Eq. (27) the quantity  $\delta N$  is the deviation of the number of electrons of the HOMO from its half-filling value 1. In formulas  $\delta N$  can be written as the difference between  $(N - \text{Int}[N])$  and 1. In Fig. 6 we show  $G_s$  and  $G$  versus  $v_g$  for different values of the broadening parameter  $\gamma$ . The value  $\gamma = 1.8$  meV is the one employed in Fig. 4 of I. For small  $\gamma$  we clearly see a pattern similar to that of Fig. 3 in I: if  $N$  is close to an odd number then  $G_s$  exhibits a Kondo plateau. The dynamical xc correction of Eq. (27) suppresses this plateau and yields the correct CB pattern.

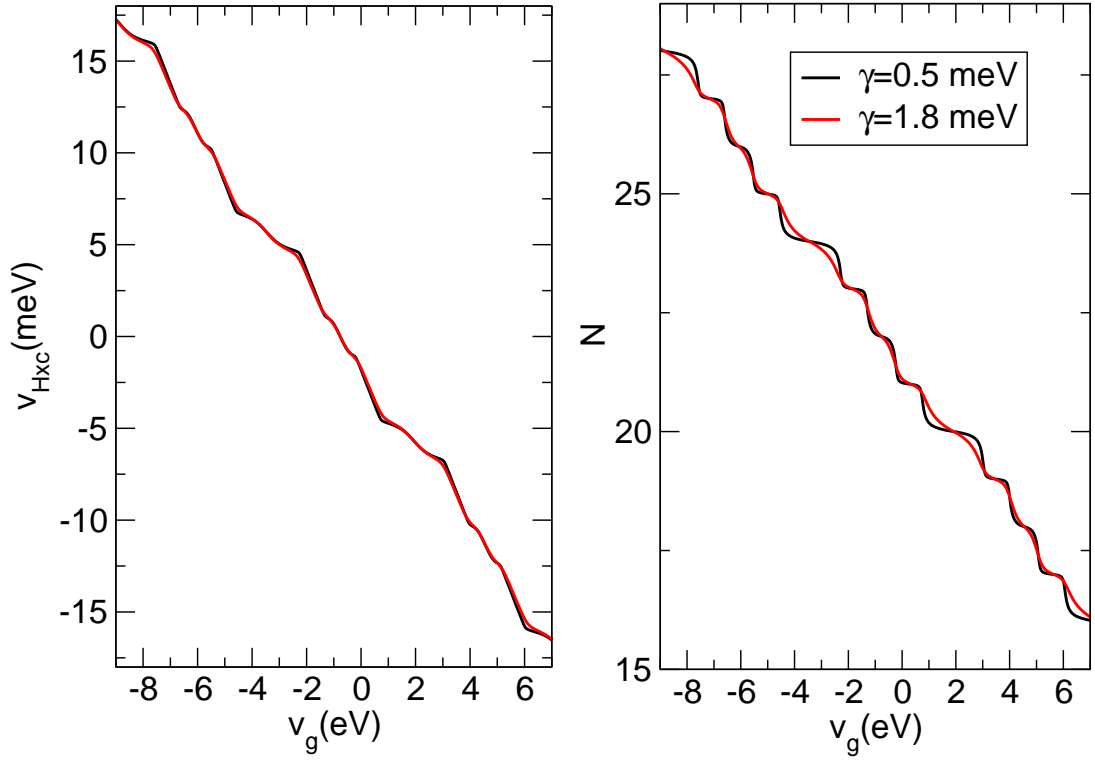


FIG. 5. KS Hxc potential (Eq. (21)) and number of electrons on the SWNT quantum dot for different values of the coupling  $\gamma$  to the leads.

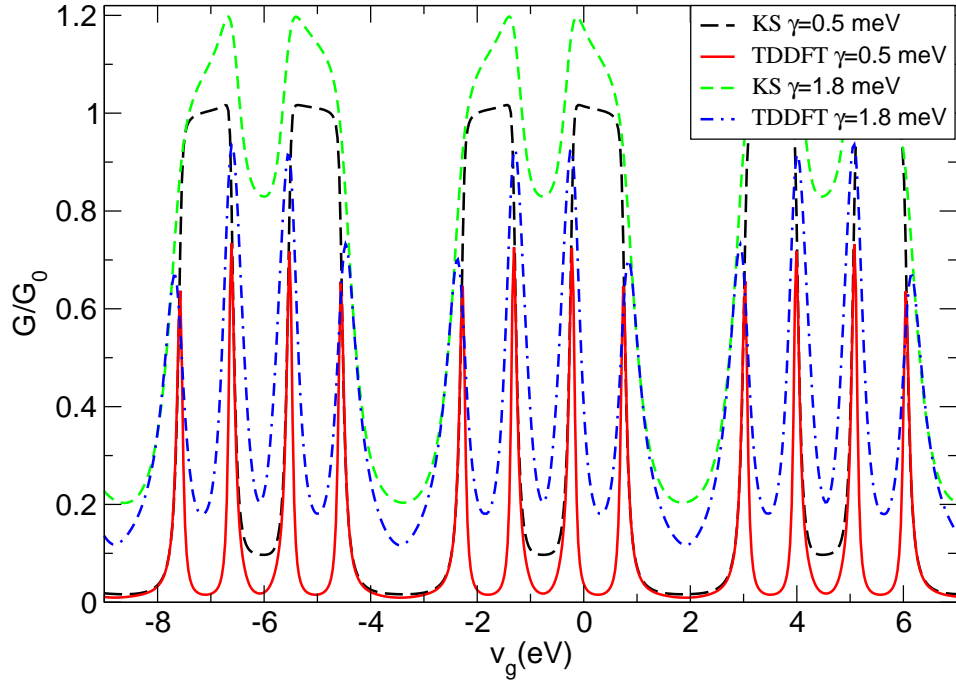


FIG. 6. KS and TDDFT corrected conductances for the SWNT quantum dot for different values of the coupling  $\gamma$  to the leads.